DALTON

# Synthesis, structural characterisation, electron paramagnetic resonance and magnetic studies of homoleptic copper complexes of pyridonate ligands†

**Alexander J. Blake,[a] Craig M. Grant,[a] Eric J. L. McInnes,[b] Frank E. Mabbs,[b] Paul E. Y. Milne,[a] Simon Parsons,[a] Jeremy M. Rawson[a] and Richard E. P. Winpenny *,[a]**

[a] *Department of Chemistry, The University of Edinburgh, West Mains Road, Edinburgh EH9 3JJ, UK*
[b] *EPSRC c.w. EPR Service Centre, Department of Chemistry, The University of Manchester, Manchester M13 9PL, UK*

Three homoleptic copper(II) complexes have been prepared which feature 6-halogen-substituted 2-pyridonate ligands $[\{Cu_2(xhp)_4\}_n]$ ($n$ = 1, xhp = 6-chloro- or 6-bromo-2-pyridonate; $n$ = 2, xhp = 6-fluoro-2-pyridonate). X-Ray structural analysis of the complexes showed that for the chlorine- and bromine-substituted derivatives a dinuclear complex forms where the xhp ligands are arranged to give a dimeric unit with idealised $D_{2d}$ symmetry. For the fluorine-substituted ligand smaller steric requirements allow rearrangement to occur to give dinuclear units with approximate $C_{4v}$ symmetry, which can then dimerise giving tetrametallic molecules. The Cu · · · Cu contacts within these species are around 2.5 Å, and to investigate the nature of the Cu · · · Cu interaction variable-temperature EPR and magnetic studies were carried out. These revealed strong antiferromagnetic exchange between the $S = \frac{1}{2}$ centres; EPR also revealed a weak interdimer exchange which was not evident from susceptibility measurements.

Dinuclear copper(II) complexes are among the most widely studied polymetallic compounds. One cause of this attention is their relevance to the active sites of some metalloproteins. A second reason is that they are the simplest metal complexes which show co-operative magnetic phenomena, involving two $S = \frac{1}{2}$ centres with negligible orbital contributions to their magnetism. This second strand has produced several classic pieces of magnetochemistry, including the Bleaney–Bowers equation,[1] and the oft-quoted magnetostructural correlation in hydroxo-bridged dimers first described by Hatfield[2] and extended by Kahn and co-workers,[3] and since applied to other superexchange systems.[4,5]

When there is a clear superexchange path, for example *via* μ-OH groups, the mechanism of magnetic exchange in dinuclear copper species is well understood, mainly due to the aforementioned magnetostructural correlations. The nature of the exchange in dinuclear complexes where there is no such path has been more controversial.[6] There are two possible mechanisms: direct interaction between copper centres, perhaps involving a δ overlap, or an interaction through several ligand orbitals. Recently the latter explanation has become more favoured. Here we report an investigation of the magnetism and EPR spectroscopy of a series of dinuclear copper complexes where the superexchange path clearly appears to be ligand mediated. The results also illustrate that EPR spectroscopy can, under certain circumstances, give information about very weak exchange coupling which is not noticeable from susceptibility measurements.

## Experimental

6-Chloro-2-pyridone (Hchp) and copper salts were obtained from Aldrich and used without further purification. 6-Bromo-2-pyridone (Hbhp) was synthesised by a published procedure[7] and 6-fluoro-2-pyridone (Hfhp) by a modification of that procedure.[8] Sodium salts of pyridones were prepared by reaction of the latter with sodium methoxide in methanol, followed by evaporation to dryness. All solvents were used as obtained.

The NMR spectra were recorded on a Bruker AM-360 MHz spectrometer in $CDCl_3$ but in all cases no signals were observed. Mass spectra were obtained using fast atom bombardment on samples in a 3-nitrobenzyl alcohol matrix, UV/VIS/NIR spectra on a Shimadzu UV-160A spectrophotometer.

### Preparation of compounds

**$[Cu_2(chp)_4]$ 1.** Hydrated copper nitrate (1.21 g, 5 mmol) and Na(chp) (1.5 g, 10 mmol) were ground together to give a dark red paste. Addition of dichloromethane (250 $cm^3$) gave a dark red solution, which was filtered to remove unreacted copper nitrate. Evaporation to dryness gave an intensely coloured red solid which was recrystallised by diffusion of diethyl ether vapour into a dichloromethane solution. Yield of crystalline solid 60% (Found: C, 37.1; H, 1.8; N, 8.6. Calc.: C, 37.4; H, 1.8; N, 8.7%). No significant peaks were observed by FAB mass spectrometry.

**$[Cu_2(bhp)_4]$ 2.** This complex was prepared in a similar manner to that of **1**. The crystalline material obtained was brown. Yield 82% (Found: C, 29.6; H, 1.5; N, 6.8. Calc.: C, 29.3; H, 1.5; N, 6.8%). FAB mass spectrum (significant peaks, possible assignments): $m/z$ 474, $[Cu_2(bhp)_2]$; 411, $[Cu(bhp)_2]$.

**$[\{Cu_2(fhp)_4\}_2]$ 3.** This complex was prepared in a similar manner to that of **1**. The crystalline material obtained was dark green. Yield 89% (Found: C, 43.1; H, 2.3; N, 9.8. Calc.: C, 41.7; H, 2.1; N, 9.7%). FAB mass spectrum: $m/z$ 926, $[Cu_4(fhp)_6]$; 814, $[Cu_4(fhp)_5]$; 799, $[Cu_2(fhp)_6]$; 702, $[Cu_4(fhp)_4]$; 639, $[Cu_3(fhp)_4]$; 590, $[Cu_4(fhp)_3]$; 575, $[Cu_2(fhp)_4]$; 350, $[Cu_2(fhp)_2]$; 289, $[Cu(fhp)_2]$; 240, $[Cu_2(fhp)]$; 176, $[Cu(fhp)]$.

### Crystallography

Crystal data and data collection and refined parameters for compounds **1–3** are given in Table 1, selected bond lengths and angles in Tables 2 and 3.

† *Non-SI unit employed:* G = $10^{-4}$ T.

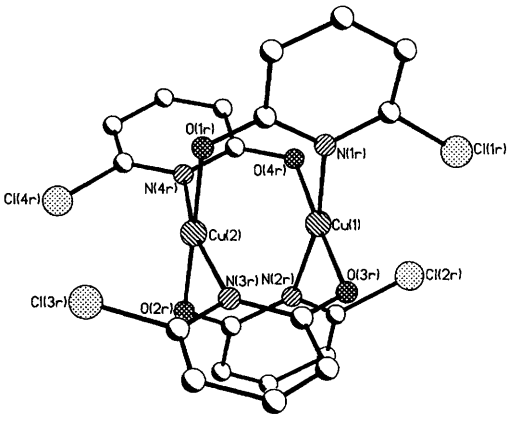


**Fig. 1** Structure of compound **1** in the crystal showing the atomic numbering scheme; **2** is isostructural

**Data collection and processing.** Data were collected for all compounds on a Stoë Stadi-4 four-circle diffractometer equipped with an Oxford Cryosystems low-temperature device[9] operating at 150 K with graphite-monochromated Mo-K$\alpha$ radiation ($\lambda$ = 0.710 73 Å), $\omega$–2$\theta$ scans, using on-line profile fitting[10] for **1** and **2**. Data were corrected for Lorentz-polarisation factors. Semiempirical absorption corrections based on azimuthal measurements[11] were applied for all compounds. A further correction using DIFABS[12] was applied to **2** to allow for large absorption effects due to Br atoms (maximum, minimum corrections: 1.237, 0.742).

**Structure analysis and refinement.** All structures were solved by the heavy-atom method using SHELXS 86[13] which revealed the positions of the copper atoms. All other non-H atoms were found in subsequent $\Delta F$ maps. Structures **1** and **2** were refined on $F$ using SHELX 76,[14] with all non-H atoms anisotropic in **1** and Cu, Br, Cl and O anisotropic in **2**. Structure **3** was refined on $F^2$ using SHELXL 93[15] with all non-H atoms anisotropic. Hydrogen atoms were included in all refinements at idealised positions (C–H 0.96 Å), with fixed isotropic thermal parameters for **1** and **3** [$U$(H) = 0.04 Å$^2$] and isotropic thermal parameters tied to that of their parent C atom for **2** [$U$(H) = 1.2 $U$(C) Å$^2$ for ring carbons, 1.5 $U$(C) Å$^2$ for methyl groups].

Atomic coordinates, thermal parameters, and bond lengths and angles have been deposited at the Cambridge Crystallographic Data Centre (CCDC). See Instructions for Authors, *J. Chem. Soc., Dalton Trans.*, 1996, Issue 1. Any request to the CCDC for this material should quote the full literature citation and the reference number 186/200.

### Magnetic measurements

Variable-temperature magnetic measurements in the region 5–300 K were made on a SQUID susceptometer (Quantum Design) on samples sealed in gelatin capsules. In all cases diamagnetic corrections for the sample holders were applied to the data. Diamagnetic corrections for the samples were determined from Pascal's constants[16] and literature values.[17] The observed and calculated data were refined using in-house software.[18]

### EPR Measurements

All EPR spectra were recorded using a Bruker ESP300E spectrometer. X-Band (*ca.* 9.5 GHz) measurements from room temperature to 100 K utilised a Bruker ER4116DM resonator with a BVT2000 variable-temperature unit; an Oxford instruments ESR910 cryostat was used for temperatures below 100 K. Q-Band measurements (*ca.* 34.2 GHz) used a Bruker ER5106QT resonator with an ER4118VT cryostat (295–100 K) or an ER4118CF cryostat (100–4.2 K). Computer simulations of spectra were performed using in-house software.[19] Complex **1** was initially reported to be EPR silent as a dichloromethane glass at 77 K,[20] however on re-examination we found both **1** and **2** give very weak signals in $CH_2Cl_2$ at X-band and 140 K and collection of multiple scans was necessary to give acceptable signal-to-noise ratios.

## Results and Discussion

### Structures

Much structural chemistry of pyridonate ligands has been described, chiefly by the groups of Cotton and Garner. This has recently been reviewed.[21] This work concentrated on second- and third-row transition metals, with the only 3d metal extensively studied being chromium.[22–25] Some dinuclear compounds have been reported for copper.[20,26–29] Here we show that the structural chemistry of copper with pyridonate ligands has features similar to those observed for 4d and 5d metals, and for chromium.

Compounds **1** and **2** are isostructural. In both, two copper atoms are quadruply bridged by pyridonate ligands with the two copper co-ordination sites identical (Fig. 1). Each copper is bound to two nitrogen and two oxygen donors which are arranged in a *trans* fashion. This leads to a molecule with idealised $D_{2d}$ symmetry, with the $S_4$ axis coincident with the Cu · · · Cu vector. The structures are very similar to that found by Cotton *et al.*[22] for $[Cr_2(chp)_4]$. This contrasts with the structure observed for $[Cu_2(ehp)_4(dmf)_2]$[26] **4** (ehp = the anion of 3-ethyl-2-pyridone, dmf = dimethylformamide) which has the two N- and two O-donors arranged about both copper sites in a *cis* geometry, leading to a molecule with idealised $C_{2h}$ symmetry.

The most notable feature in both compounds **1** and **2** is the short Cu · · · Cu contact. In **1** it is 2.4991(11) Å, while in **2** it is 2.5111(25) Å. These are among the shortest contacts known between copper(II) centres in dinuclear species, although longer than some contacts between copper(I) atoms and longer than contacts in trinuclear copper(II) species formed with bis(2-pyridyl)amine.[30] The reason for the short distance is probably the absence of axial ligation; for example the similar complex **4** has two molecules of dmf attached in the axial sites and a Cu · · · Cu contact of 2.550(1) Å. The small, but statistically significant, difference between **2** and **1** can also be related to this factor. In both there are long contacts to the halogen atoms in the 6 positions of the pyridonate ligand. For **1** these contacts are between 2.957(2) and 3.042(2) Å while for **2** the contacts are between 3.038(4) and 3.181(4) Å. The distances are similar but in **2** the less electronegative bromine group may have a stronger interaction with the copper centres. Similar observations have been noted by Cotton *et al.*,[31] and explain why in compounds with formal metal–metal bonds the metal–metal distance in bhp-bridged complexes is longer than the distance in the isostructural chp-bridged dimers. It is curious that a similar effect is seen in **1** and **2** where there is no formal metal–metal bond. We might also note that the strength of any direct magnetic interaction between copper orbitals should be influenced by the presence or absence of axial ligation, whereas superexchange through the ligands should not be so strongly influenced.

A further subtle difference between compounds **1** and **2** is caused by the close proximity of the halo groups. In **1** the shortest intramolecular Cl · · · Cl distance is 3.685(3) Å, while in **2** the shortest Br · · · Br distance is 3.765(7) Å; both are close to the sum of van der Waals radii for the elements. A repulsive interaction is therefore expected and is the cause of distortions of the copper co-ordination sphere. The N–Cu–N angles are all reduced to *ca.* 166°, from the ideal 180° for a *trans* angle. Related effects are seen in the Cu–N and Cu–O bonds. The Cu–O bond distances, which average 1.929 Å in **1** and 1.903 Å in **2**,

**Table 1** Experimental data for the X-ray diffraction studies of compounds **1**–**3**

| | **1** | **2** | **3** |
|---|---|---|---|
| Formula | $C_{20}H_{24}Cl_4Cu_2N_4O_4$ | $C_{20}H_{24}Br_4Cu_2N_4O_4 \cdot CH_2Cl_2 \cdot H_2O$ | $C_{40}H_{48}Cu_4F_8N_8O_8$ |
| $M$ | 641 | 934 | 1174 |
| Crystal system | Orthorhombic | Monoclinic | Tetragonal |
| Space group | $P2_12_12_1$ | $P2_1/c$ | $I4_1/a$ |
| $a$/Å | 15.394(2) | 9.000(13) | 24.385(6) |
| $b$/Å | 15.8925(13) | 13.985(8) | $=a$ |
| $c$/Å | 18.497(2) | 22.53(2) | 13.838(5) |
| β/° | | 95.39(4) | |
| $U$/Å$^3$ | 4526 | 2824 | 8225 |
| $Z$ | 8 | 4 | 8[a] |
| $D_c$/g cm$^{-3}$ | 1.88 | 2.16 | 1.86 |
| Crystal size/mm | 0.27 × 0.19 × 0.04 | 0.85 × 0.40 × 0.15 | 0.50 × 0.09 × 0.05 |
| Crystal shape and colour | Deep red plate | Deep red lath | Yellow-brown needle |
| μ/mm$^{-1}$ | 2.40 | 7.35 | 2.14 |
| Unique data | 2701 | 3682 | 3589 |
| Observed data, $F > 4\sigma(F)$ | 2036 | 2282 | 2282 |
| Parameters | 307 | 223 | 307 |
| Maximum Δ/σ ratio | 0.049 | 0.001 | 0.001 |
| $R,R'$[b] | 0.0440, 0.0494 | 0.0574, 0.0691 | — |
| $R1,wR2$[c] | — | — | 0.0576, 0.1500 |
| Weighting scheme,[d] $w^{-1}$ | $\sigma^2(F_o) + 0.0005(F_o)^2$ | $\sigma^2(F_o) + 0.000\,67(F_o)^2$ | $\sigma^2(F_o^2) + (0.0535P)^2$ |
| Goodness of fit | 0.952 | 1.154 | 1.044 |
| Largest residuals/e Å$^{-3}$ | 0.54, −0.56 | 1.26, −1.24 | 0.57, −0.59 |

[a] The molecule lies on an inversion centre. [b] SHELX 76. Refinement on $F$; $R$ and $R'$ on observed data. [c] SHELXL 93. Refinement on $F^2$; $R1$ based on observed data, $wR2$ on all unique data. [d] $P = \frac{1}{3}[\max(F_o^2, 0) + 2F_c]$.

**Table 2** Selected bond lengths (Å) and angles (°) for compounds **1** and **2**

| | **1** | **2** |
|---|---|---|
| Cu(1)···Cu(2) | 2.4991(11) | 2.5111(25) |
| Cu(1)–N(1r) | 2.000(6) | 2.051(12) |
| Cu(1)–N(2r) | 2.007(6) | 2.019(12) |
| Cu(1)–O(3r) | 1.932(5) | 1.899(10) |
| Cu(1)–O(4r) | 1.926(5) | 1.908(10) |
| Cu(2)–O(1r) | 1.933(5) | 1.908(10) |
| Cu(2)–O(2r) | 1.924(5) | 1.896(10) |
| Cu(2)–N(3r) | 2.028(6) | 2.053(12) |
| Cu(2)–N(4r) | 2.020(6) | 2.021(12) |
| N(1r)–Cu(1)–N(2r) | 167.45(23) | 164.8(5) |
| N(1r)–Cu(1)–O(3r) | 89.36(22) | 87.7(4) |
| N(1r)–Cu(1)–O(4r) | 88.24(22) | 90.3(4) |
| N(2r)–Cu(1)–O(3r) | 90.74(21) | 90.7(5) |
| N(2r)–Cu(1)–O(4r) | 91.79(21) | 92.1(5) |
| O(3r)–Cu(1)–O(4r) | 177.44(20) | 175.9(4) |
| O(1r)–Cu(2)–O(2r) | 179.26(20) | 177.7(4) |
| O(1r)–Cu(2)–N(3r) | 90.64(21) | 88.5(4) |
| O(1r)–Cu(2)–N(4r) | 90.00(21) | 89.2(4) |
| O(2r)–Cu(2)–N(3r) | 89.66(21) | 91.0(5) |
| O(2r)–Cu(2)–N(4r) | 89.86(21) | 91.8(5) |
| N(3r)–Cu(2)–N(4r) | 167.13(23) | 165.1(5) |

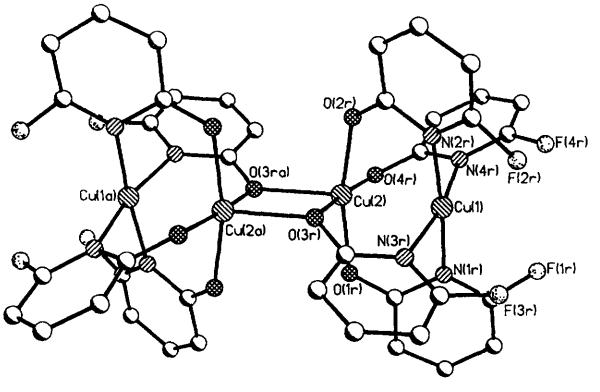


**Fig. 2** Structure of compound **3** in the crystal showing the atomic numbering scheme

**Table 3** Selected bond lengths (Å) and angles (°) for compound **3**

| | | | |
|---|---|---|---|
| Cu(1)···Cu(2) | 2.5425(14) | Cu(2)···Cu(2a) | 3.116(2) |
| Cu(1)–N(1r) | 1.987(6) | Cu(1)–N(2r) | 1.986(6) |
| Cu(1)–N(3r) | 2.034(6) | Cu(1)–N(4r) | 2.024(6) |
| Cu(2)–O(1r) | 1.968(5) | Cu(2)–O(2r) | 1.966(5) |
| Cu(2)–O(3r) | 1.971(5) | Cu(2)–O(4r) | 1.927(5) |
| Cu(2)–O(3ra) | 2.177(5) | | |
| N(1r)–Cu(1)–N(2r) | 175.0(2) | N(3r)–Cu(1)–N(4r) | 168.0(2) |
| N(1r)–Cu(1)–N(3r) | 89.5(2) | N(1r)–Cu(1)–N(4r) | 90.7(2) |
| N(2r)–Cu(1)–N(3r) | 89.3(2) | N(2r)–Cu(1)–N(4r) | 89.4(2) |
| O(1r)–Cu(2)–O(2r) | 164.4(2) | O(3r)–Cu(2)–O(4r) | 171.9(2) |
| O(1r)–Cu(2)–O(3r) | 88.3(2) | O(1r)–Cu(2)–O(4r) | 97.5(2) |
| O(1r)–Cu(2)–O(3ra) | 97.2(2) | O(2r)–Cu(2)–O(3r) | 88.6(2) |
| O(2r)–Cu(2)–O(4r) | 89.6(2) | O(2r)–Cu(2)–O(3ra) | 97.2(2) |
| O(3r)–Cu(2)–O(3ra) | 82.7(2) | O(4r)–Cu(2)–O(3ra) | 105.3(2) |
| Cu(2)–O(3r)–Cu(2a) | 97.3(2) | | |

are shorter than in the sterically less crowded **4** where this distance averages 1.959 Å. The Cu–N bonds are longer in **1** and **2**, averaging 2.014 and 2.036 Å respectively, compared with 2.000 Å in **4**. The difference is only statistically significant between **2** and **4**.

Complex **3** isolated from reaction of Na(fhp) with copper nitrate, in an exactly analogous manner to the synthesis of **1** and **2**, shows the importance of such halogen–halogen repulsions in determining structure. It crystallises as a centrosymmetric tetranuclear molecule which can be described as a dimer of dinuclear species (Fig. 2). Within the dinuclear unit the two copper co-ordination sites are quite distinct; one bound exclusively to N-donor atoms from fhp ligands, and one site bound only to O-donors. This arrangement leads to all four fluorine substituents pointing in the same direction, which appears somewhat unfavourable for steric reasons, but allows two additional Cu–O bonds between dinuclear units. For the smallest halogen it seems that the halogen–halogen repulsion term is smaller than the energy gain from forming an additional Cu–O bond per dimer. The repulsion is lessened a little by a 'twist' of the ligands with an average N–Cu–Cu–O torsion angle of 19° compared with a similar 'twist' of only 4° in **2**.

The first co-ordination site is bound to four N atoms in a

**Table 4** Magnetic data derived from susceptibility studies for compounds **1**–**4**

| Compound | Formula | $J/cm^{-1}$ | $g$ | ρ | Ref. |
|---|---|---|---|---|---|
| **1** | $[Cu_2(chp)_4]$ | 370 | 2.14[a] | 0.04 | *b* |
| **2** | $[Cu_2(bhp)_4]$ | 360 | 2.10 | 0.10 | *b* |
| **3** | $[\{Cu_2(fhp)_4\}_2]$ | 345 | 2.11 | 0.09 | *b* |
| **4** | $[Cu_2(ehp)_4(dmf)_2]$ | 395 | 2.15 | — | 26 |

[a] From single-crystal EPR study. [b] This work.

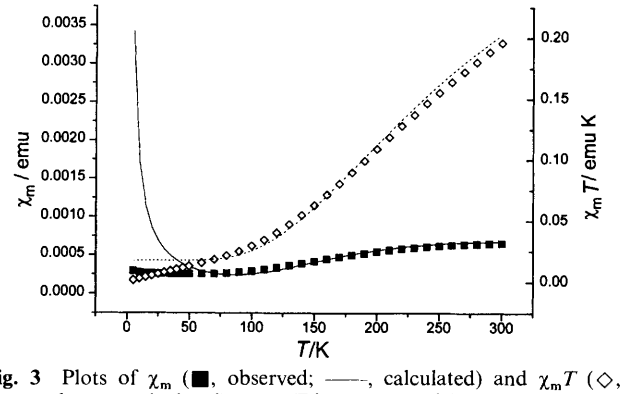


**Fig. 3** Plots of $\chi_m$ (■, observed; ——, calculated) and $\chi_m T$ (◇, observed; – – –, calculated) *versus* $T$ for compound **1**

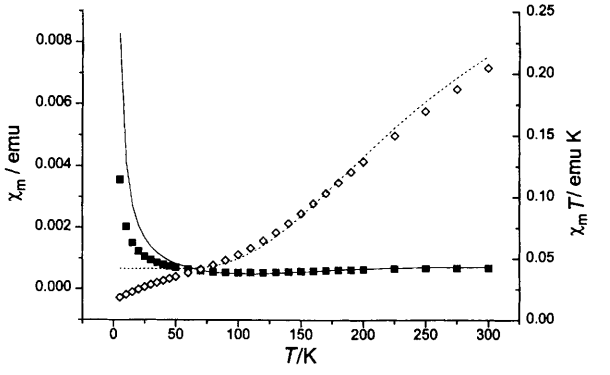


**Fig. 4** Plots of $\chi_m$ and $\chi_m T$ *versus* $T$ for compound **2**. Details as in Fig. 3

regular square-planar array. The Cu–N distances are very similar to those in compound **1**. The second co-ordination site is bound to five O atoms, with a distorted square-pyramidal geometry; it is *via* the axial oxygen atom [O(3a)] of the square pyramid that the dinuclear units are linked. The equatorial Cu–O distances are slightly longer than in **1** with the bond to the axial O atom yet longer at 2.177(5) Å. The presence of an axial donor group leads to a intradimer Cu(1) • • • Cu(2) distance of 2.5425(14) Å, longer than in **1** or **2**. The interdimer interaction Cu(2) • • • Cu(2a) distance is 3.116(2) Å. The *trans* N–Cu–N and O–Cu–O angles in **3** are all smaller than 180°, indicating a more general strain in the molecule compared with **1** and **2** where only the N–Cu–N angles were reduced.

Again, the tendency of complexes of the fhp ligand to crystallise with all four ligands orientated in the same direction has been noted for chromium chemistry.[24] The complex $[Cr_2(fhp)_4(thf)]$ (thf = tetrahydrofuran) has two unique chromium sites; one bound to four N atoms, the second to five O atoms, the fifth coming from co-ordinated thf. Here, in the absence of co-ordinating solvents, the additional M–O bond is formed by dimerisation of the dinuclear units.

The packing of di- and tetra-nuclear units of compounds **1**–**3** within the crystals shows no strong intermolecular interactions. In each case the closest contacts are between halogen substituents. In **1** these involve direct interactions between chloride substituents in neighbouring dimers, leading to a chain-like motif in the structure. In **2** there are no direct interdimer contacts in this range (shortest direct contact 3.85 Å), but there are some interactions with molecules of $CH_2Cl_2$ solvate at 3.41 Å. Finally in **3** the closest contacts are directly between fluorine atoms in neighbouring tetranuclear molecules at *ca.* 2.83 Å. Whether these contacts have any structural significance is debatable.

## Physical studies

The most obvious difference between compounds **1**–**3** and previously reported copper pyridonate complexes is their solubility. Indeed many copper complexes with structures related to copper(II) acetate are highly insoluble in all but the most polar solvents, whereas **1**–**3** are soluble in chlorinated hydrocarbons. It is probable that the presence of groups in the 6 position of the pyridonate ring prevents extended oligomerisation of the units and hence increases solubility.

Unfortunately, although more spectroscopic and physical studies are possible because of the greater solubility, the results are in general negative. None of compounds **1**–**3** give any resolved signals by NMR spectroscopy, unlike hexa- and octanuclear complexes of pyridonate ligands which we have reported previously.[32,33] The UV/VIS/NIR spectra, recorded in $CH_2Cl_2$, show bands due to intraligand π–π* transitions for each complex, and additionally an absorption band at *ca.* 400 nm for each species, with an absorption coefficient of around 1000 $dm^3\ mol^{-1}\ cm^{-1}$ per $Cu_2$ unit. Absorptions of this wavelength have frequently been regarded as diagnostic of the presence of Cu • • • Cu contacts within dimers. For each complex a further band is observed at lower energy and with lower intensity. For **1** and **2** the band is near 520 nm, while for **3** it is at 697 nm. The lower intensity suggests that these bands are d–d transitions.

The FAB mass spectra were also recorded for all three compounds. The molecular ion was not observed for any of the species, although significant fragment peaks were observed for **3**.

## Magnetic studies

Magnetic studies of compounds **1**–**3** were carried out over the temperature range 5–300 K. For each case the behaviour of an exchanged-coupled system, expressed in terms of the exchange Hamiltonian (1), could be modelled using the Bleaney–Bowers equation [1] (2), where $g$ is the average $g$ value, $J$ is the exchange

$$\mathscr{H}_{ex} = J\cdot\hat{S}_1\cdot\hat{S}_2 \quad (1)$$

$$\chi = \frac{Ng^2\beta^2}{3k(T-\theta)}\cdot\frac{1}{1+\frac{1}{3}\exp(J/kt)}(1-\rho)+\frac{Ng^2\beta^2\rho}{4kT} \quad (2)$$

integral and ρ is the percentage of monomeric ($S = \frac{1}{2}$) impurity; θ is a term which allows for interdimer interactions. The values of the parameters used in modelling the data are given in Table 4 with data for **4**.

An unambiguous interpretation of the susceptibility measurements was not obtained. It proved impossible to fit both the high-temperature region and the region between 5 and 50 K, therefore we have concentrated our efforts on the former as the majority of the information concerning $g$ and $J$ is contained in the range above 50 K. For **1** we used the $g$ value obtained from EPR studies rather than allowing this parameter to vary. For **2** and **3** the $g$ value was allowed to vary between 2.1 and 2.2 during the fitting procedure. In all three cases it was necessary to include a factor for a monomeric impurity in the model.

For compounds **1** and **2** good fits were achieved which indicate a strong antiferromagnetic exchange and a singlet–triplet gap of around 360 $cm^{-1}$. Plots of $\chi_m$ and $\chi_m T$ per $Cu_2$ unit against $T$ for **1** and **2** are shown in Figs. 3 and 4 respectively.

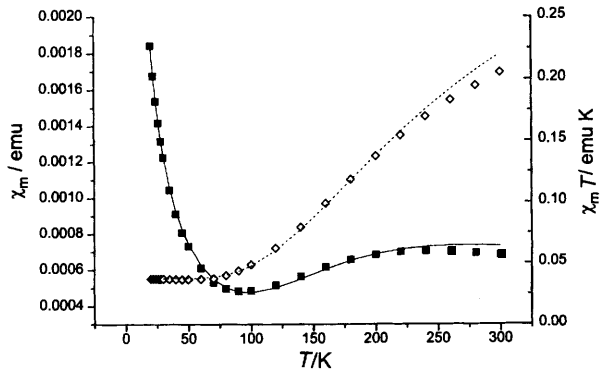


**Fig. 5** Plots of $\chi_m$ and $\chi_m T$ *versus* $T$ for compound **3**. Details as in Fig. 3

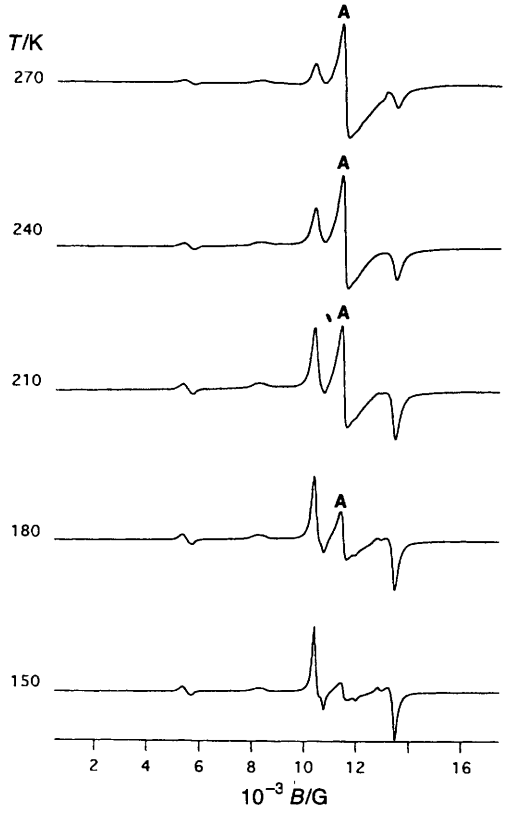


**Fig. 6** Variable-temperature (270 to 120 K) Q-band powder EPR spectra of compound **1**. Feature **A** at $g_{eff} = 2.1$ is due to intermolecular interactions (see text); all other features are due to isolated spin-triplet states

At low temperature the observed and calculated data diverge slightly. For neither **1** nor **2** is an interdimer term θ necessary to model the data adequately. While the values obtained for all parameters are sensible, the insensitive response of the sample makes the value for the exchange integral somewhat ill defined. Slightly better agreement between measured and calculated behaviour could be obtained with a singlet–triplet gap of around 400 $cm^{-1}$ but with $g$ values of 2.00 which are not remotely consistent with the EPR studies.

For compound **3** a very good fit is achieved with a $g$ value of 2.1 and a $J$ value of 345 $cm^{-1}$. No interdimer exchange term is required to fit the data, which may initially appear surprising given the crystal structure. However if the superexchange between dinuclear units within **3** proceeds *via* the bridging O atoms then as the Cu–O–Cu bridge angle is 97.3(2)° the magnetostructural correlation of Hatfield would indicate an exchange integral of close to zero. The correlation should hold as the $Cu_2O_2$ ring is strictly planar. Furthermore the bridging O atom is in an axial position for one of the two Cu atoms bridged, and therefore almost orthogonal to the magnetic orbital; again this should result in a very small exchange integral. Plots of $\chi_m$ and $\chi_m T$ per $Cu_2$ unit against $T$ for **3** are shown in Fig. 5.

## EPR Studies

Spectra have been recorded of powdered samples of compounds **1**–**3** at both X- and Q-band. Additionally X-band spectra of **1** and **2** as frozen glasses in $CH_2Cl_2$ have been studied, and a single-crystal study of **1** at X-band has been undertaken. Full details of the single-crystal study and the detailed analysis thereof are given elsewhere.[34]

The X- and Q-band spectra of the powdered samples of compounds **1** and **2** reveal three types of resonance which show quite distinct temperature dependence (Fig. 6). At room temperature the spectrum is in each case dominated by a broad, almost isotropic resonance at *ca.* $g_{eff} = 2.1$, with a second set of much weaker features indicative of a spin-triplet state. On cooling **1** or **2** to 100 K the broad resonance at $g_{eff} = 2.1$ decreases dramatically in intensity, and is not observed below 120 K at Q-band. Although the features due to the triplet state increase in amplitude on cooling this is due to a narrowing of linewidth, and the overall intensities decrease as would be expected for the spectrum of a thermally populated excited state, and below 40 K the features due to the triplet state disappear. The third type of resonance is due to a monomeric impurity and is first observed below 200 K for **1** and at all temperatures for **2**; this feature becomes dominant at low temperatures. The features due to the spin-triplet state and the monomer impurity are expected, however the broad, isotropic signal at $g_{eff} = 2.1$ is unusual. In particular the dramatic fall in intensity of this signal at lower temperatures is inconsistent with a paramagnetic impurity and indicates that it arises from intermolecular interactions between spin-triplet molecules in the solid state; such a resonance has previously been reported for $[Cu_2(O_2CEt)_4(p\text{-}ClC_6H_4NH_2)_2]$.[35]

A single-crystal study[34] of compound **1** gave the spin-Hamiltonian parameters for the triplet state of this species as $g_{zz} = 2.30, g_{xx} = 2.07, g_{yy} = 2.05, |D| = 0.275\ cm^{-1}$ and $|\lambda|$ (*i.e.* $E/D) = 0.01$, with the $z$ direction coincident with the Cu • • • Cu vector ($|D|$ and $E$ are the zero-field splitting parameters). These parameters can then be used to simulate the powder spectra at both X- and Q-band. As the powder spectrum of **2** is essentially identical to that of **1** then the spin-Hamiltonian parameters must be very similar. These values are similar to those reported for **4**.[29]

The availability of a suitable single crystal allowed intra- and inter-dimer exchange interactions to be derived from line-shape analysis.[36,37] The detail of this analysis is reported elsewhere.[34] For compound **1** the variation of linewidth indicates a singlet–triplet gap of 360 ± 20 $cm^{-1}$ and an interdimer exchange of around 0.15 $cm^{-1}$. This singlet–triplet gap is in good agreement with that obtained from susceptibility measurements. The relative magnitudes of the interdimer exchange and the zero-field splitting lead to the observation of the $g_{eff} = 2.1$ resonance; if the interdimer exchange were much larger than the zero-field splitting then a broad isotropic resonance would be observed at all temperatures. The spectra of **3** provide sufficient evidence of this in that the $g_{eff} \approx 2.1$ feature does not diminish with cooling and dominates the spectra at all temperatures. The 'dimer of dimers' structure of **3** presumably provides a much more efficient pathway for interdimer interactions for **3** than **1** or **2**, however we could not detect this difference by magnetic measurements, only through EPR studies.

The X-band frozen-glass spectra of both compounds **1** and **2** ($CH_2Cl_2$, 140 K) reveal hyperfine structure on the feature due to the $\Delta M_s = 2$ transition. The seven-line pattern confirms that the dimer structure is retained in solution, and $A_{Cu}$ is measured at 70 G for both **1** and **2**.

## Conclusion

The synthetic and structural results reported here add to the small number of structurally characterised pyridonate complexes of 3d metals. The structural differences between the tetranuclear complex **3** and **1** and **2** also show how seemingly trivial modifications of the pyridonate ligand can lead to rather more dramatic changes in structure; however the most important results reported here relate to the magnetic and EPR properties of the complexes.

Neither susceptibility nor EPR measurements alone serve unambiguously to derive the singlet–triplet gap in these complexes, however the combination of the techniques used for **1** is more persuasive than either techique could be alone. The values found for **1** and **2** are around 365 $cm^{-1}$, somewhat smaller than that obtained for **4**. Given the absence of axial ligands we might have expected a more dramatic change in this energy gap, and certainly we would have expected the value to be greater than that for **4** if the exchange interaction is directly between copper d orbitals. Therefore we believe this is good experimental evidence for superexchange *via* the pyridonate ligands being the dominant mechanism for the antiferromagnetic coupling in these species. The value obtained for **3** is slightly smaller than that for **1** or **2**.

The EPR results are consistent with the X- and Q-band powder spectra of compound **4** reported by Goodgame *et al.*,[29] and with the Hamiltonian parameters derived therefrom. It was noted[29] that the value observed for $|D|$ of 0.287 $cm^{-1}$ (compared with 0.275 $cm^{-1}$ found here) fell between the values found for dinuclear copper species with exclusively oxygen donors {*e.g.* $|D| = 0.34$ $cm^{-1}$ for $[Cu_2(MeCO_2)_4(H_2O)_2]$} and those with exclusively N-donors {*e.g.* $|D| = 0.12$ $cm^{-1}$ for $[Cu_2(ade)_4]\cdot 4H_2O$, where ade = the anion of adenine]. No further comment was made.

There are two contributions to $D$, a dipolar contribution ($D^{dip}$, which can be related to the Cu • • • Cu distance) and the anisotropic exchange ($D^{exch}$) which involves exchange between the ground state of one copper and an excited state of the second.[38] The trend in the magnitude of $|D|$ can be explained as due to variation in $D^{exch}$ which is explicable in simple ligand-field terms. For weak-field donors such as oxygen the excited states are nearer in energy to the ground state, leading to a large value for $D^{exch}$ (and hence $|D|$), as found for copper acetate. For a stronger-field donor such as nitrogen the energy gap to the excited states is larger, and this leads to a smaller value for $D^{exch}$, as found for the complex of adenine. For pyridonate ligands therefore, which have a mixture of N- and O-donors, an intermediate value for $D^{exch}$ is sensible. A similar trend is observed for the $g$ values of these complexes.

The EPR results also illustrate the importance of studies at a range of temperatures. At room temperature the $g_{eff} \approx 2.1$ signal might have been assigned to a monomeric impurity. A measurement at liquid-nitrogen temperature would also have contained a strong signal in this region, this time genuinely due to the presence of monomer rather than to intermolecular exchange. Thus the interpretation of spectra at only two temperatures could have led to a spurious assignment of the room-temperature feature.

## Acknowledgements

We are grateful to the EPSRC for studentships (to C. M. G. and P. E. Y. M.), a post-doctoral fellowship (to S. P.) and for funding for a diffractometer and SQUID susceptometer in Edinburgh, and for funding the Multi-frequency EPR Centre in Manchester. We are also grateful to the Leverhulme Trust for a post-doctoral fellowship (to J. M. R.).

## References

1 B. Bleaney and K. Bowers, *Proc. R. Soc. London, Ser. A*, 1952, **214**, 451.
2 W. E. Hatfield, in *Magneto-Structural Correlations in Exchange Coupled Systems*, eds. R. D. Willett, D. Gatteschi and O. Kahn, *NATO ASI Ser., Sect. C*, 1985, **140**, 555.
3 M. F. Charlot, S. Jeannin, Y. Jeannin, O. Kahn, J. Lucrèce-Abaul and J. Martin-Frère, *Inorg. Chem.*, 1979, **18**, 1675.
4 K. K. Nanda, L. K. Thompson, J. N. Bridson and K. Nag, *J. Chem. Soc., Chem. Commun.*, 1994, 1337.
5 S. S. Tandon, L. K. Thompson, M. E. Manuel and J. N. Bridson, *Inorg. Chem.*, 1994, **33**, 5555; L. K. Thompson, S. S. Tandon and M. E. Manuel, *Inorg. Chem.*, 1995, **34**, 2356.
6 J. Catterick and P. Thornton, *Adv. Inorg. Radiochem*, 1977, **20**, 291.
7 G. R. Newkome, J. Broussard, S. K. Staires and J. D. Sauer, *Synthesis*, 1974, 707.
8 A. J. Blake, C. M. Grant, S. Parsons and R. E. P. Winpenny, *J. Chem. Soc., Dalton Trans.*, 1995, 1765.
9 J. Cosier and A. M. Glazer, *J. Appl. Crystallogr.*, 1986, **19**, 105.
10 W. Clegg, *Acta Crystallogr., Sect. A*, 1981, **37**, 22.
11 A. C. T. North, D. C. Phillips and F. S. Mathews, *Acta Crystallogr., Sect. A*, 1968, **24**, 351.
12 N. Walker and D. Stuart, DIFABS, program for applying empirical absorption corrections, *Acta Crystallogr., Sect. A*, 1983, **39**, 158.
13 G. M. Sheldrick, SHELXS 86, *Acta Crystallogr., Sect. A*, 1990, **46**, 467.
14 G. M. Sheldrick, SHELX 76, University of Cambridge, 1976.
15 G. M. Sheldrick, SHELXL 93, University of Göttingen, 1993.
16 C. J. O'Conner, *Prog. Inorg. Chem.*, 1982, **29**, 203.
17 *Handbook of Chemistry & Physics*, 70th edn., ed. R. C. Weest, CRC Press, Boca Raton, FL, 1994, p. E134.
18 J. M. Rawson, unpublished work.
19 *Electron Paramagnetic Resonance of d Transition Metal Compounds*, eds. F. E. Mabbs and D. Collison, Elsevier, Amsterdam, 1992, ch. 16.
20 A. J. Blake, R. O. Gould, P. E. Y. Milne and R. E. P. Winpenny, *J. Chem. Soc., Chem. Commun.*, 1992, 522.
21 J. M. Rawson and R. E. P. Winpenny, *Coord. Chem. Rev.*, 1995, **139**, 313 and refs. therein.
22 F. A. Cotton, P. E. Fanwick, R. H. Niswander and J. C. Sekutowski, *J. Am. Chem. Soc.*, 1978, **100**, 4725.
23 F. A. Cotton, W. H. Ilsley and W. Kaim, *Inorg. Chem.*, 1980, **19**, 1453.
24 F. A. Cotton, L. R. Falvello, S. Han and W. Wang, *Inorg. Chem.*, 1983, **22**, 4106.
25 L. Akhter, W. Clegg, D. Collison and C. D. Garner, *Inorg. Chem.*, 1985, **24**, 1725.
26 Y. Nishida and S. Kida, *Bull. Chem. Soc. Jpn.*, 1985, **58**, 383.
27 S. K. Yeh, D. S. Liaw and S. M. Peng, *Bull. Inst. Chem., Acad. Sin.*, 1987, **34**, 49.
28 S. Emori, I. Okana and Y. Muto, *Bull. Chem. Soc. Jpn.*, 1972, **45**, 3717.
29 D. M. L. Goodgame, Y. Nishida and R. E. P. Winpenny, *Bull. Chem. Soc. Jpn.*, 1986, **59**, 344.
30 L.-P. Wu, P. Field, T. Morrisey, C. Murphy, P. Nagle, B. Hathaway, C. Simmons and P. Thornton, *J. Chem. Soc., Dalton Trans.*, 1990, 3835.
31 F. A. Cotton, T. Ren and J. L. Eglin, *J. Am. Chem. Soc.*, 1990, **112**, 3439.
32 A. J. Blake, R. O. Gould, C. M. Grant, P. E. Y. Milne, D. Reed and R. E. P. Winpenny, *Angew. Chem., Int. Ed. Engl.*, 1994, **33**, 195.
33 A. J. Blake, C. M. Grant, C. I. Gregory, S. Parsons, J. M. Rawson, D. Reed and R. E. P. Winpenny, *J. Chem. Soc., Dalton Trans.*, 1995, 163.
34 E. J. L. McInnes, F. E. Mabbs, C. M. Grant, P. E. Y. Milne and R. E. P. Winpenny, *J. Chem. Soc., Faraday Trans.*, in the press.
35 V. V. Gavrilov, Y. V. Yablokov, L. N. Milkova and A. V. Ablov, *Phys. Status Solidi B*, 1971, **45**, 603.
36 J. S. Valentine, A. J. Silverstein and Z. G. Soos, *J. Am. Chem. Soc.*, 1974, **96**, 97.
37 M. T. Jones and D. B. Chestnut, *J. Chem. Phys.*, 1963, **38**, 1311.
38 *Electron Paramagnetic Resonance of d Transition Metal Compounds*, eds. F. E. Mabbs and D. Collison, Elsevier, Amsterdam, 1992, ch. 15.

*Received* 3rd *May* 1996; *Paper* 6/03119F